RSC Advances

ROYAL SOCIETY OF CHEMISTRY

www.rsc.org/advances

Journal Name

COMMUNICATION

Self-Healing Elastomers Assembly Towards Three-Dimensional Shape Memory Devices

Received 00th January 20xx,
Accepted 00th January 20xx

DOI: 10.1039/x0xx00000x

www.rsc.org/

Xianqi Feng, [a,b] Gongzheng Zhang, [a] Bo Xu, [a] Haoyang Jiang, [a] Quanming Bai [a] and Huanjun Li* [a]

The superior self-healing elastomers were readily prepared by free-radical copolymerization of Methoxyethyl acrylate (*MEA*) and *N,N*-dimethylacrylamide (*DMAA*). The synergistic interaction between the shape memory effect and the reversible weak hydrogen bonds lead to the excellent self-healing properties and high mechanical strength of the elastomers. By taking advantage of the two outstanding performances, we demonstrated that various novel two-dimensional (2D) and three-dimensional (3D) shape memory devices can be designed delicately on the basis of self-healing mediated assembly of the elastomers as building blocks. This assembly method to combine self-healing and shape memory properties might open a promising avenue for design and fabrication of 3D complex-shape smart devices.

Self-healing polymeric materials are under intense investigation due to their self-repair ability which would significantly extend material's lifespan, improve product safety, and ensure sustainability[1,2]. For these purposes, a variety of approaches have been developed to obtain self-healing elastomers[3]. Over the past decade, two kinds of conceptual self-healing, namely extrinsic system[4-6] and intrinsic system[7,8], have been reported. The last one based on reversible bonds has recently attracted much more attention not only due to their automatic and intrinsic healing nature, but also for their easily modification and wide applications[9]. The reversible bonds including non-covalent[10-12] or dynamic covalent bonds[13-15] can reversibly rupture and reform to provide self-healing capability. For example, with heat[16,17] or light irradiation[18-20], the reversible bonds at damaged areas can be re-established, thus resulting in the polymer chains to diffuse and re-entangle above the glass transition temperature (T_g), hence enabling polymer to achieve healing.

To date, much effort has been devoted to stiff materials and composites. However, limited approaches have been developed to design self-healing elastomers. Such materials are highly desirable towards replacement of conventional rubber as biomedical devices[21,22], stretchable conductive wires[23,24], protective coatings[25,26], sealing agents[27], etc. For the reported self-healing elastomers[28-30], the complicated molecular design and time-consuming synthesis process were required usually in order to achieve high healing efficiency. In addition, these self-healing elastomers generally exhibited weak mechancial strength, which limits their practical applications[22]. Hence, developing a simple method to obtain intrinsic self-healing elastomers with both high healing efficiency and high strength still remain a great challenge.

Recently, shape memory polymers (SMPs), as a smart material which can recover to the permanent shape from a temporary one upon an external stimulus[31,32], have been developed to improve the self-healing process by closing mechanical damage or crack based on shape memory effect[33-35]. For example, Mather and coworkers reported a new strategy of healing mechanism based on shape memory assisted self-healing polymers (SMASH), which are contributed to diffusion and rebonding of polymer chain at damage areas above T_g[36]. Sodano and coworker demonstrated the self-healing of the thermoresponsive polyurethanes by using shape memory effect to close cracks without external forces[33]. However, the healing process is only effective for the minor crack or scratch in the specimens, and is unsuitable for complete cutting specimens. Thus, exploiting new types of SMPs with the cut self-healing ability is important for the practical application. On the other hand, many elastomers showed the excellent shape memory performance, which is expected to improve their self-healing efficiency. Furthermore, taking advantage of self-healing elastomers with shape memory behavior as building blocks is of particular interest for creating 3D responsive material structures, especially 3D shape memory devices, which are difficult to be fabricated by conventional polymer processing methods[37].

Herein, we described a facile method for the rapid fabrication of intrinsic self-healing elastomers by combining free-radical copolymerization of two common monomers in aqueous solution and subsequent dry treatment. We reasoned that the self-healing capability of the elastomers results from the synergistic interaction

---

[a] *School of Chemical Engineering and Environment, Beijing Institute of Technology, Beijing 100081, P. R. China. E-mail: Lihj@bit.edu.cn.*

[b] *College of Chemical and Materials Engineering, Yanching Institute of Technology, Langfang 065201, P. R. China.*

† Electronic Supplementary Information (ESI) available: Experimental procedure, elatomers characterization, and summary of mechanical and self-healing properties of the elastomers. See DOI: 10.1039/x0xx00000x

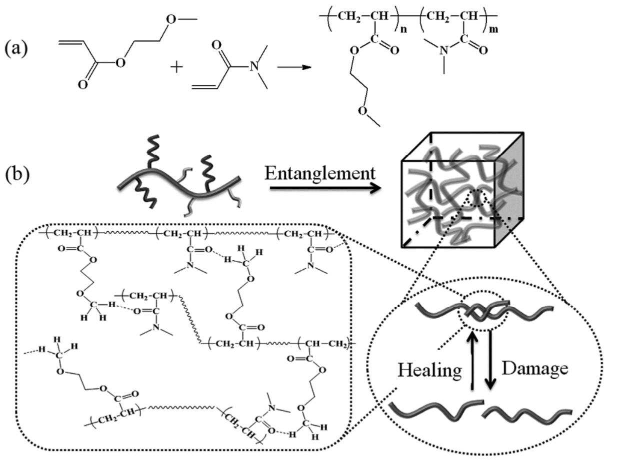

Figure 1. (a)Synthetic route of MD copolymer; (b) Schematic illustration of the self-healing process of MD copolymer elastomers.

between shape memory effect and the reversible weak hydrogen bonds. Meanwhile, the elastomers show excellent shape memory effect and high mechanical strength. Moreover, the healable ability of the elastomers enables the cut rod-like specimens which act as building blocks to assembly into versatile 2D and 3D shape memory devices. We expect that the complex 3D responsive structures constructed by self-healing mediated assembly will be useful in applications that explore high value added devices of stimuli-responsive materials.

The detailed synthesis procedures for the elastomers can be found in experiment sections. Briefly, the appropriate amount of 2-Methoxyethyl acrylate (MEA) and N,N-dimethylacrylamide (DMAA) were added in ultrapure water with N_2 gas bubbling for 1 h to remove any soluble O_2. After vigorous stirring for another 15 min, the solution was cooled to 0 ℃ before catalyst (TEMED, 8 μL) and initiator (0.01 g in 0.5 ml water) were added. Finally, the final mixture was transferred to a tailored glass tube and polymerized at 60 ℃ for 12 h to obtain the wet samples. The obtained samples were washed thoroughly with distilled water to remove the unreacted monomer and other impurities. The resulting samples were subsequently dried at room temperature for 24 h followed by drying for 24 h at 80 ℃ under vacuum in order to obtain the elastomers (Figure 1a described the preparation scheme). MEA and DMAA are chosen as two monomers of copolymerization (The T_gs of PMEA and PDMAA are -34 ℃ and 124 ℃ , respectively)[38]. The codes for the resultant samples were defined as MDx by the mole fraction of DMAA, where $x = 100 \times ([\mathrm{DMAA}]) / ([\mathrm{DMAA}] + [\mathrm{MEA}])$. The shape memory behavior in MD copolymer system is likely contributed to the physical crosslinks by polymer chain entanglements, which set the permanent shape and the switching segments (motion of polymer chains) serve as reversible domains with a thermoreversible phase transition based on T_g. For our self-healing MD system, the pendent amide carbonyl group and methoxy group are capable of forming dynamic networks based on the weak hydrogen bonds interactions, having both weak hydrogen bond donor and hydrogen bond acceptor functionality[39]. When the elastomer is subjected to external damage (e.g., cut), the polymer chains diffusion across the fractured interfaces can be act as the primary driving force for repairing, and the polymer chain entanglment interactions assisted with weak hydrogen bonds bear the responsibility of restoration for the mechanical strength. Although the interactions are very weak, the pervasive net-work of dynamic weak hydrogen bonds can afford mechanical robustness on the relevant timescales (as illustrated in Figure 1b)[40]. Therefore, with the assistance of weak hydrogen bonds, diffusion and entanglement of polymer backbones affords spontaneous self-healing behavior.

The presence of hydrogen bonds within the polymer was confirmed by FT-IR spectra and temperature-variable FT-IR spectra. As shown in Figure 2a, the spectra were dominated by two sets of absorption bands (1728 cm^{-1}, 1635 cm^{-1}) corresponding to stretching vibrations of ester carbonyl group and amide carbonyl group. It is evident that the peak of amide carbonyl clearly shifts to 1635 cm^{-1} from 1645 cm^{-1} (neat PDMAA)[41]. One possible cause for this shift is the interchain dipolar interactions between the dipolar groups (amide carbonyl, methoxy group) of adjacent molecular chains. In order to further confirm and understand the nature of specific interactions between the methoxy group and carbonyl group, the temperature-variable FTIR spectroscopy for MD50 film was conducted, as shown in Figure 2b. With increasing temperature, the C=O stretching band shifts to large wavenumbers, and from 1654 cm^{-1} to 1658 cm^{-1} for amide carbonyl group, due to the broken of the weak hydrogen bonds between amide carbonyl group and methoxy group. All results suggested the existence of weak hydrogen bond interactions between the methoxyl group and amide carbonyl group, and the weak hydrogen bond interactions could improve self-healing ability due to its reversible characteristic.

With the increasing of DMAA molar fraction, the glass transition temperature of the resulting copolymers have also changed as confirmed by their dynamic mechanical analysis (DMA) tests[42]. In specific, the polymer of MD45 has a T_g of 14.2 ℃, while the T_g of MD50 and MD55 increased to 22.2 ℃and 35.4 ℃, respectively (Figure 2b). The T_g value of MD50 was close to that of differential scanning calorimetry in Figure S2. It is worth noting that the tanδ curves of all samples depended on temperature display a

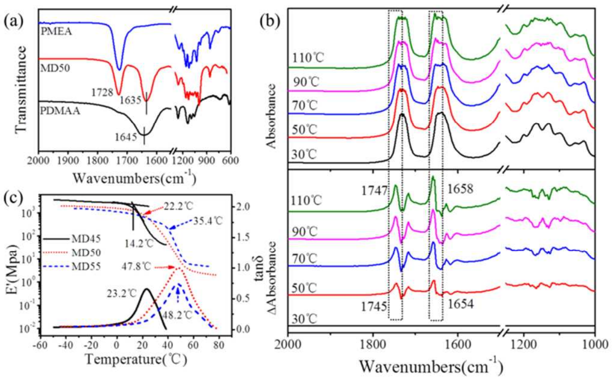

Figure 2. (a) FT-IR spectra of the PMEA, PDMAA, and MD50; (b) original FT-IR spectra, difference spectra of MD50 film as temperature increased from 30 ℃ to 110 ℃; (c) DMA profiles of MD45, MD50, and MD55 elastomers.

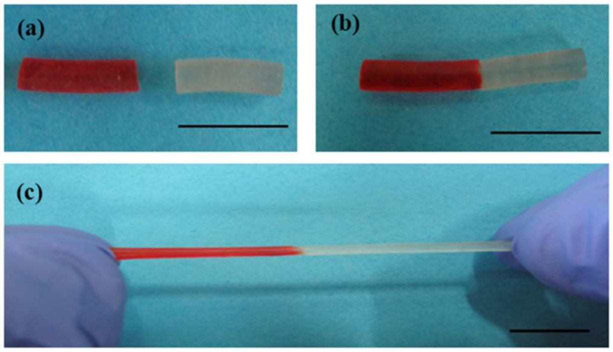

Figure 3. Photographs showing the self-healing behavior of MD50 elastomer: (a) two isolated blocks; (b) the fractured surfaces were contacted and healed; (c) the healed sample can bear stretching to about 250% strain without failure. The scale bar was 1 cm for all images.

sharp peak, which is required for a good SMP using temperature as the switch model[43]. Since the lower glass transition temperature, the MD copolymers can be reversibly molded into various shapes at elevated temperature. Besides, as mentioned above, the motion of the polymer chains above T_g would provide the primitive driving force for self-healing behavior. And we found that such MD copolymers can self-heal at elevated temperature without any need of healing agent.

The self-healing phenomenon was shown with the pictures in Figure 3. The cylindrical sample of 3 mm diameter was cut into completely two separate blocks using a razor blade, one of which contains a red pigment for visualization, and then the two halves were bought into contact. After healing for 12 h at 90 ℃, the physical interface between the damaged surfaces were completely healed. The joint between the two blocks is strong enough to sustain large stretching (~250% strain) without failure. The healing process of the cut sample was observed using optical microscope, and the representative images were shown in Figure S3. The results indicated that the shape memory effect of elastomers during healing process favored the closure of the cracks and the following self-healing by chain's diffusion and entanglement assisted with weak hydrogen bonds.

To further quantitatively evaluate the self-healing performance of the MD system, tensile stress-strain tests were performed on the virgin and self-healed specimens of MD45, MD50, and MD55. The mechanical properties and self-healing efficiency of samples are summarized in Table S1. As shown in Figure 4a, with increasing of molar ratio of DMAA (from 45% to 55%), the tensile stress rapid increased from 5.0 MPa to 14.4 MPa, and the Young's modulus increased from 35.0 MPa to 52.0 MPa, while the elongation at break decreased from 620% to 375%. The tensile tests for three healed samples revealed a similar trend, the fracture stress and the Young's modulus increased, while the elongation at break significantly decreased. For all healing samples, stress-strain curves show characteristic thermoplastic elastomer behavior and follow closely the shapes of the original uncut samples, and the optimal healing of up to 98.2% recovery of tensile strength relative to a virginal sample for MD50 elastomer. Comprehensively, MD45 is the most extensible and MD55 is the stiffest and strongest, but MD50 seems to have the most impressive self-healing property. It is worth noting that the tensile strength of our self-healing elastomers is superior of that of most reported self-healing elastomers with less than 5.0 MPa. Even though some previously reported self-healing polymers owned high strength but they were not elastic.

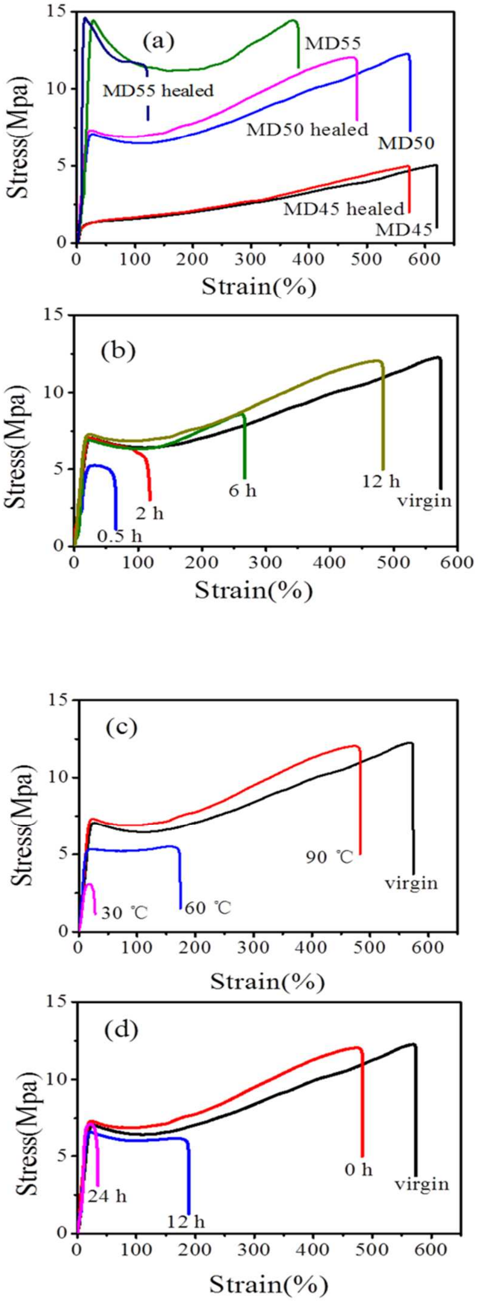

Figure 4. The typical tensile stress-strain curves of virgin and self-healing samples with different molar ratio of DMAA (a), healing times (b), healing temperature (c), and waiting time before fracture surfaces being putting together (d).

To get more insight into the underlying mechanism of self-healing, we investigated the impact of a number of parameters on the self-healing performance such as healing time, healing temperature, and waiting time of the cut specimens before being brought into contact. Initially, longer healing times lead to better healing. As shown in Figure 4b, the healing efficiency significantly improved with extending the healing time, and optimal healing of up to 98.2% recovery of tensile strength of virgin sample. Indeed, after healing for 2 h, the MD50 sample can be healed up to about 60% of its original tensile strength, which indicated that more than half self-healing process occurred within the two hours after bringing the two cut pieces back in contact.

For self-healing polymer materials, factors which promote diffusion of polymer chains lead to the increase of self-healing efficiency. As shown in Figure 4c, the fracture stress, elongation, and self-healing efficiency of MD50 remarkably increased with the raising of temperature due to the accelerating motion of polymer chains. Like most of self-healing materials that rely on hydrogen bonds, the self-healing efficiency of our samples of MD50 elastomer rapid decreased when the two fractured surfaces are left apart for as short as several hours. As illustrated in Figure 4d, several samples of MD50 were cut and kept apart for different durations, and the self-healing efficiencies were subsequently tested after being healed. The fracture stress dropped to about 7.0 MPa (about 60% of tensile strength of virginal sample) after two fractured surfaces were left apart for 24 h, while the elongation at break dropped rapidly(only recovery of about 3% of its virgin sample). This property could be contributed to the fast recombination of weak hydrogen bonds, at the same time, hinder the mobile of polymer chains, leading the decay of self-healing efficiency.

The excellent self-healing capability of the elastomers enables applications such as multi-dimensional assembly of devices, especially constructing 3D responsive materials structures. In Figure 5 a series of one-dimensional (1D), 2D, and 3D shape memory devices from self-healing mediated assembly of MD50 elastomer as building blocks were illustrated. Figure 5a shown that the 1D permanent rod-like sample (sizes of 20 mm×3 mm) could be healed and assembled above T_g after being cut into two halves. The reversible transition between the permanent shape and two temporary shapes could be observed. The two temporary shape were obtained by bending to “S” shape and stretching to about 250% at 50 ℃ and cooling to room temperature. when heat to 50 ℃ again, the recovery of the permanent shape occurred in one minute. Figure 5b showed the self-healing and shape memory behaviors of triangle device constructed using three cut elastomer segments. The assembled triangle was subjected to stretch with three different directions and become larger reverse triangle. Then the reverse triangle was fixed as the temporary shape at ambient temperature, and could recover to the original shape after heating to 50 ℃. Most importantly, we further demonstrated that 3D cubic device could also be constructed from self-healing mediated assembly by using 12 building blocks, which were obtained by cutting the two long rod-like elastomers (see Figure 5c). The assembled 3D cube based on self-healing process without any healing agent was compressed into irregular temporary shape at 50 ℃, and the temporary shape was fixed by cooling to room temperature. The permanent cubic shape was recovered gradually with the heating time, and almost accomplished recovery in 75 s. In addition, it should be noted that the assembled cube can bear load of 400 times the weight of itself without failure (Figure S5). Thus, the self-healing mediated assembly method enables the construction of one dimensional structure into versatile three dimensional devices, especially 3D shape memory devices, which is otherwise difficult to do with conventional fabrication method. These results suggest that the developed MD50 copolymer elastomer may have a great potential applications ranging from self-healing materials to 3D responsible devices.

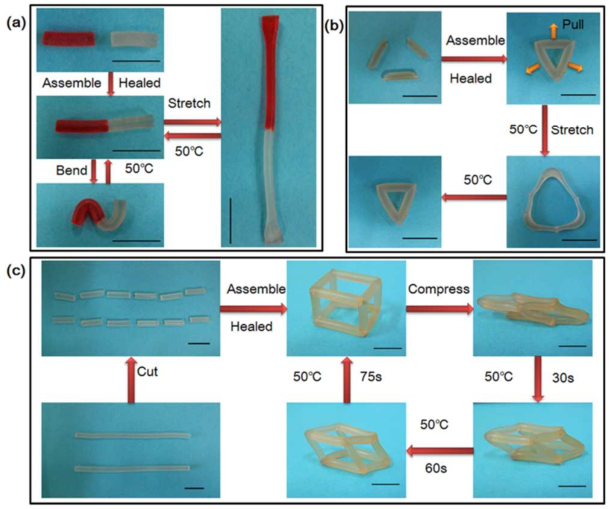

Figure 5. The self-healing mediated multi-dimensional assembly of MD50 copolymer elastomers: a) 1D assembly, the rod-like samples was cut into two pieces and subsequent assembly into 1D rod-like structure, which was bent and stretched at 50 ℃; b) 2D assembly, the rod-like sample was cut into three building blocks and assembled into a 2D triangle shape, which was stretched with three different directions for shape fixation at room temperature and then recovered to the initial shape at 50 ℃; c) 3D assembly, two rod-like samples were cut into 12 building blocks, which were used to assembly into a cubic device. The assembled cube was compressed into the temporary shape at 50 ℃, and the temporary shape was fixed at ambient temperature and the permanent cubic shape was recovered gradually at 50 ℃ in 75 s. The scale bar was 1cm for all images.

In summary, we have developed a simple and effective strategy for designing novel self-healing elastomers with superior shape memory performance and excellent mechanical properties, based on facile copolymerization of two common monomers MEA and DMAA. It is worth noting that compared with the previous reported self-healing elastomers, our MD elastomers after healed shows higher strength and modulus. Also, the resultant elastomer exhibits excellent self-healing properties with 98% recovery. Furthermore, by combining high healing efficiency and high strength of the elastomers, a series of 1D, 2D, and 3D shape memory devices can be easily constructed from self-healing mediated assembly of MD50 elastomer as building blocks. In particular, we have demonstrated the first example of 3D shape memory device based on assembly of self-healing elastomers. These high strength self-healing elastomers and shape memory devices would have potential applications in soft smart materials.

Acknowledgement

This work was supported by the Natural Science Foundation of China (21174017), the Beijing Municipal Natural Science Foundation of China (2102040). the Cultivation Project for Technology Innovation Program of BIT (2011CX01032).

Notes and references

1 D. Mozhdehi, S. Ayala, O. R. Cromwell and Z. B. Guan, *J. Am. Chem. Soc.*, 2014, **136**, 16128-16131.
2 Y. Z. Gao, Q. Luo, S. P. Qiao, L. Wang, Z. Y. Dong, J. Y. Xu and J. Q. Liu, *Angew. Chem. Int. Edit.*, 2014, **53**, 9343-9346.
3 Y. Yang and M. W. Urban, *Chem. Soc. Rev.*, 2013, **42**, 7446-7467.
4 S. R. White, N. R. Sottos, P. H. Geubelle, J. S. Moore, M. R. Kessler, S. R. Sriram, E. N. Brown and S. Viswanathan, *Nature*, 2001, **409**, 794-797.
5 A. Latnikova, D. O. Grigoriev, J. Hartmann, H. Mohwald and D. G. Shchukin, *Soft Matter*, 2011, **7**, 369-372.
6 J. L. Wietor and R. P. Sijbesma, *Angew. Chem. Int. Edit.*, 2008, **47**, 8161-8163.
7 H. Chen, X. Ma, S. Wu and H. Tian, *Angew. Chem. Int. Edit.*, 2014, **53**, 14149-14152.
8 C. Wang, N. Liu, R. Allen, J. B. H. Tok, Y. P. Wu, F. Zhang, Y. S. Chen and Z. N. Bao, *Adv. Mater.*, 2013, **25**, 5785-5790.
9 Y. L. Chen, A. M. Kushner, G. A. Williams and Z. B. Guan, *Nat. Chem.*, 2012, **4**, 467-472.
10 H. Kuroki, I. Tokarev, D. Nykypanchuk, E. Zhulina and S. Minko, *Adv. Funct. Mater.*, 2013, **23**, 4593-4600.
11 J. Hentschel, A. M. Kushner, J. Ziller and Z. B. Guan, *Angew. Chem. Int. Edit.*, 2012, **51**, 10561-10565.
12 A. Vidyasagar, K. Handore and K. M. Sureshan, *Angew. Chem. Int. Edit.*, 2011, **50**, 8021-8024.
13 C. Wang, N. Liu, R. Allen, J. B. Tok, Y. Wu, F. Zhang, Y. Chen and Z. Bao, *Adv. Mater.*, 2013, 25, 5785-5790.
14 Y. Hisamatsu, S. Banerjee, M. B. Avinash, T. Govindaraju and C. Schmuck, *Angew. Chem. Int. Edit.*, 2013, **52**, 12550-12554.
15 C. Zeng, H. Seino, J. Ren, K. Hatanaka and N. Yoshie, *Macromolecules*, 2013, **46**, 1794-1802.
16 M. Arslan, B. Kiskan and Y. Yagci, *Macromolecules*, 2015, **48**, 1329-1334.
17 Y. K. Bai, Y. Chen, Q. H. Wang and T. M. Wang, *J. Mater. Chem. A*, 2014, **2**, 9169-9177.
18 L. Huang, N. Yi, Y. Wu, Y. Zhang, Q. Zhang, Y. Huang, Y. Ma and Y. Chen, *Adv. Mater.*, 2013, **25**, 2224-2228.
19 1D. Habault, H. Zhang and Y. Zhao, *Chem. Soc. Rev.*, 2013, **42**, 7244-7256.
20 Z. Wei, J. H. Yang, Z. Q. Liu, F. Xu, J. X. Zhou, M. Zrínyi, Y. Osada and Y. M. Chen, *Adv. Funct. Mater.*, 2015, **25**, 1352-1359.
21 B. C. Tee, C. Wang, R. Allen and Z. Bao, *Nat. nanotechnol.*, 2012, **7**, 825-832.
22 J. Lessing, S. A. Morin, C. Keplinger, A. S. Tayi and G. M. Whitesides, *Adv. Funct. Mater.*, 2015, **25**, 1418-1425.
23 Z. B. Yang, J. Deng, X. L. Chen, J. Ren and H. S. Peng, *Angew. Chem. Int. Edit.*, 2013, **52**, 13453-13457.
24 Y. K. Song and C. M. Chung, *Polym. Chem.*, 2013, **4**, 4940-4947.
25 Y. K. Song, Y. H. Jo, Y. J. Lim, S. Y. Cho, H. C. Yu, B. C. Ryu, S. I. Lee and C. M. Chung, *ACS Appl. Mater. Inter.*, 2013, **5**, 1378-1384.
26 E. Abdullayev, V. Abbasov, A. Tursunbayeva, V. Portnov, H. Ibrahimov, G. Mukhtarova and Y. Lvov, *Acs Appl. Mater. Inter.*, 2013, **5**, 4464-4471.
27 K. M. Lewis, D. Spazierer, P. Slezak, B. Baumgartner, J. Regenbogen and H. Gulle, *J. Biomater. Appl.*, 2014, **29**, 780-788.
28 L. Yang, Y. Lin, L. Wang and A. Zhang, *Polym. Chem.*, 2014, **5**, 153-160.
29 R. Martin, A. Rekondo, A. Ruiz de Luzuriaga, G. Cabañero, H. J. Grande and I. Odriozola, *J. Mater. Chem. A*, 2014, **2**, 5710-5715.
30 C. E. Yuan, M. Z. Rong and M. Q. Zhang, *Polymer*, 2014, **55**, 1782-1791.
31 P. Agarwal, M. Chopra and L. A. Archer, *Angew. Chem. Int. Edit.*, 2011, **50**, 8670-8673.
32 A. Lendlein, H. Y. Jiang, O. Junger and R. Langer, *Nature*, 2005, **434**, 879-882.
33 Y. Heo and H. A. Sodano, *Adv. Funct. Mater.*, 2014, **24**, 5261-5268.
34 G. Q. Li, O. Ajisafe and H. Meng, *Polymer*, 2013, **54**, 920-928.
35 M. Wei, M. Zhan, D. Yu, H. Xie, M. He, K. Yang and Y. Wang, *ACS Appl. Mater. Inter.*, 2015, **7**, 2585-2596.
36 X. Luo and P. T. Mather, *ACS Macro Lett.*, 2013, **2**, 152-156.
37 C. Ma, T. Li, Q. Zhao, X. Yang, J. Wu, Y. Luo and T. Xie, *Adv. Mater.*, 2014, **26**, 5665-5669.
38 K. Haraguchi, K.Murata and T.Takehisa, *Macromolecules* 2012, **45**, 385-391.
39 C. R. Jones, P. K. Baruah, A. L. Thompson, S. Scheiner, M. D. Smith, *J. Am. Chem. Soc.* 2012, **134**, 12064-12071.
40 C. Rest, M. J. Mayoral, K. Fucke, J. Schellheimer, V. Stepanenko and G. Fernandez, *Angew. Chem. Int. Ed.* **2014**, 53, 700-705.
41 N. Spegazzini, H. W. Siesler and Y. Ozaki, *J. Phys. Chem. A* 2012, **116**, 7797-7808.
42 Z. W. He, N. Satarkar, T. Xie, Y. T. Cheng and J. Z. Hilt, *Adv. Mater.* 2011, **23**, 3192-3196.
43 R. C. Zhang, T. Z. Yan, B. Lechner, K. Schroter, Y. Liang, B. H. Li, F. Furtado and P. C. Sun, K. Saalwachter, *Macromolecules* 2013, **46**, 1841-1850.